Microenvironment and Immunology

Cancer Research

Metastatic Growth from Dormant Cells Induced by a Col-I–Enriched Fibrotic Environment

Dalit Barkan[1], Lara H. El Touny[1], Aleksandra M. Michalowski[1], Jane Ann Smith[3], Isabel Chu[1], Anne Sally Davis[2], Joshua D. Webster[1], Shelley Hoover[1], R. Mark Simpson[1], Jack Gauldie[3], and Jeffrey E. Green[1]

Abstract

Breast cancer that recurs as metastatic disease many years after primary tumor resection and adjuvant therapy seems to arise from tumor cells that disseminated early in the course of disease but did not develop into clinically apparent lesions. These long-term surviving, disseminated tumor cells maintain a state of dormancy, but may be triggered to proliferate through largely unknown factors. We now show that the induction of fibrosis, associated with deposition of type I collagen (Col-I) in the *in vivo* metastatic microenvironment, induces dormant D2.0R cells to form proliferative metastatic lesions through β1-integrin signaling. *In vitro* studies using a three-dimensional culture system modeling dormancy showed that Col-I induces quiescent D2.0R cells to proliferate through β1-integrin activation of SRC and focal adhesion kinase, leading to extracellular signal-regulated kinase (ERK)–dependent myosin light chain phosphorylation by myosin light chain kinase and actin stress fiber formation. Blocking β1-integrin, Src, ERK, or myosin light chain kinase by short hairpin RNA or pharmacologic approaches inhibited Col-I–induced activation of this signaling cascade, cytoskeletal reorganization, and proliferation. These findings show that fibrosis with Col-I enrichment at the metastatic site may be a critical determinant of cytoskeletal reorganization in dormant tumor cells, leading to their transition from dormancy to metastatic growth. Thus, inhibiting Col-I production, its interaction with β1-integrin, and downstream signaling of β1-integrin may be important strategies for preventing or treating recurrent metastatic disease. *Cancer Res; 70(14); 5706–16. ©2010 AACR.*

Introduction

Metastatic disease is the major cause of mortality for breast cancer patients and may occur years or even decades after successful treatment of the primary tumor by surgery and adjuvant therapy. Recent evidence indicates that tumor cell dissemination may be an early event in the disease process (1, 2), yet little is understood about the biological mechanisms that ensure the survival of a presumably small subset of disseminated tumor cells that lay dormant for many years. Likewise, the critical triggers that regulate the transition of dormant tumor cells into a proliferative state leading to clinical recurrence remain unknown. It has been proposed that dormant tumor cells may exist in a quiescent state for many years or, alternatively, as micrometastases whose cellular proliferation is balanced by apoptosis (3–6) and which can progress to clinical disease once an angiogenic process is activated to support continued tumor growth (7).

The microenvironment has been increasingly recognized as a critical regulator of cancer progression (5, 8–10, 11) and is thought to be a major factor determining survival and growth of disseminated tumor cells at preferential metastatic sites (12). The extracellular matrix (ECM), a key component of the microenvironment, is in immediate contact with tumor cells, regulates aspects of both normal and tumor cell functions, and provides a critical source for growth, survival, motility, and angiogenic factors that significantly affect tumor biology and progression. Alterations in the expression of ECM-related genes including fibronectin and type I collagen (Col-I) have been identified in gene expression signatures related to poor prognosis and metastases in breast cancers (13–16). Fibrotic foci with Col-I are often observed in primary tumors and lymph node metastases of breast cancer patients at high risk of recurrence (17, 18). High levels of procollagen type I, a marker for Col-I synthesis, have been identified in the serum of patients with recurrent breast cancer (19).

We have recently shown that ECM composition plays a critical role in determining whether solitary dormant tumor

Authors' Affiliations: [1]Laboratory of Cancer Biology and Genetics, National Cancer Institute and [2]Laboratory of Infectious Diseases, National Institute of Allergy and Infectious Diseases, Bethesda, Maryland; and [3]Department of Pathology and Molecular Medicine, McMaster University, Hamilton, Ontario, Canada

Note: Supplementary data for this article are available at Cancer Research Online (http://cancerres.aacrjournals.org/).

Current address for D. Barkan: Department of Biology, Faculty of Sciences, Haifa University, Haifa, Israel.

L.H. El Touny and A.M. Michalowski contributed equally to this work.

Corresponding Author: Jeffrey E. Green, Building 37, Room 4054, 37 Convent Drive, National Cancer Institute, Bethesda, MD 20892. Phone: 301-435-5193; Fax: 301-496-8709; E-mail: jegreen@nih.gov.

doi: 10.1158/0008-5472.CAN-09-2356

cells remain quiescent or begin to actively proliferate using the well-characterized D2.0R/D2A1 mammary cell line model system to study dormant versus metastatic proliferative growth (20). These cell lines derived from tumors arising from implants of the same D2 hyperplastic alveolar nodule line display distinct metastatic properties (21, 22). Whereas D2A1 cells form metastatic lesions after a few weeks in mice when disseminated to multiple sites by venous injection, D2.0R cells remain dormant for months with occasional formation of metastatic lesions. Using a modified three-dimensional culture system, we showed that the quiescent or proliferative behavior of these cells could be recapitulated *in vitro* (20, 22) and regulated by the presence of the ECM component fibronectin through the activation of β1-integrin (Intβ1). Additionally, we showed that significant alterations in cytoskeletal structure are critical for the dormant-to-proliferative switch requiring the phosphorylation of myosin light chain (MLC) by MLC kinase (MLCK).

In this study, we show *in vivo* that the prior induction of fibrosis with Col-I deposition at a metastatic site results in a dramatic Intβ1-mediated increase in proliferative, metastatic lesions of D2.0R cells, which otherwise remain dormant in normal lungs. Using the *in vitro* dormancy model, we show that the proliferative response to Col-I is mediated through Intβ1 and requires Src and focal adhesion kinase (FAK) activation, extracellular signal-regulated kinase (ERK)–dependent activation of MLCK, phosphorylation of MLC (pMLC), and actin stress fiber formation.

This is the first study to our knowledge that functionally shows that fibrosis with Col-I enrichment at the metastatic site can trigger the dormant-to-proliferative switch through Intβ1 signaling and cytoskeletal reorganization in dormant tumor cells, leading to metastatic disease. These results suggest that inhibiting growth-promoting signaling from the ECM through signaling downstream of Intβ1 may be an important strategy for preventing or treating recurrent metastatic disease.

Materials and Methods

Cell lines and culture

Mouse mammary cancer D2.0R and D2A1 cells (kindly provided by Ann Chambers, London Cancer Center, Ontario; ref. 21) were cultured as previously described in two-dimensional or three-dimensional Cultrex (BME; Trevigen, Inc.; ref. 20) or in BME mixed with neutralized rat tail collagen I (final concentration 2 mg/mL). Cell morphology was imaged by confocal microscopy (LSM-META 510 Zeiss MicroImaging, Inc.). ML-7 (Biomol International L.P.), W13 and U0126 (Calbiochem), and PP1 (Biomol International L.P) were used to inhibit MLCK, calmodulin, ERK, and Src activities, respectively. Anti-Intβ1 antibody clone 9EG7 (azide free) was used to antagonize Intβ1 function, and nonspecific IgG was used as a control (BD Biosciences). Sublines of D2.0R and D2A1 cells were generated to express green fluorescent protein (GFP) using the pSICO lentivirus (kindly provided by Tyler Jacks, Massachusetts Institute of Technology, Cambridge, MA).

Proliferation assay

Cells (2×10^3) were resuspended in 100 μL DMEM low glucose supplemented with 2% fetal bovine serum (FBS) +2% BME, or 2% FBS + BME+Col-I, respectively, and grown on 96-well plates coated with 50 μL BME or BME+ Col-I. Proliferation was measured as previously described (20). Experiments were repeated three times with eight replicates each.

Short hairpin RNA silencing experiments

Cells were transfected with PLKO-1 plasmids expressing either short hairpin RNAs (shRNA) targeting Src (shSrc; Clone ID: TRCN0000023596) or scrambled shRNA (Open Biosystems), and cultured in the three-dimensional system 48 hours later as previously described (20). Additionally, total protein extracts were isolated from the transfected cells in two-dimensional culture at 72 hours for Western blot analysis. For stable knockdown of Intβ1, cells were transduced with Mission shRNA lentiviral particles targeting either mouse Intβ1 (sh-Intβ1) or with nontarget sh-RNA (sh-NT) control (Sigma) and selected with puromycin as per the manufacturer's protocol.

Western blot

Western blot was carried out as previously described (20). The primary antibodies used were as follows: goat anti-mouse Intβ1 (0.2 μg/mL; R&D System), monoclonal antibody against Src (1:1,000; Upstate Cell Signaling Solutions), and monoclonal antibody against β-actin (1:40,000; Sigma).

Animal studies

All mice were treated in accordance with the guidelines of the Animal Care and Use of Laboratory Animals (NIH publication no. 86-23, 1985) under an approved animal protocol and in accordance with the guidelines of the Canadian Council of Animal Care.

Experimental metastasis assays. D2A1-GFP cells (1×10^6) were tail vein injected into 6- to 8-week-old female BALB/c-*nu/nu* athymic mice (Charles Rivers Laboratories). Lungs were removed 2 weeks postinjection, inflated with PBS, and analyzed by fluorescent single cell whole organ microscopy (SCOM) imaging (Leica DM IRB) as previously described (20). 100X images of the total external surface of each lung were sequentially captured and analyzed using OpenLab software (20, 23). Lungs were then frozen in Optimal Cutting Temperature compound (Sakura), and immunofluorescence was performed on frozen sections.

Induction of pulmonary fibrosis. Eight-week-old female CD1/*nu/nu* athymic mice received 5×10^8 PFU of adenoviral vector expressing either active transforming growth factor β1 (TGFβ1; Ad-TGFβ1$^{223/225}$) to induce fibrosis or adenovirus-null vector control (Ad-empty) in 20 μL PBS to the lungs as previously described (24). Twenty-one days postinfection, 1×10^6 D2.0R-GFP cells, D2.0R-GFP+nontarget shRNA or D2.0R-GFP+Intβ1 shRNA cells were tail vein injected to nontreated mice or mice receiving Ad-empty or Ad-TGFβ-1$^{223/225}$. Lungs were removed 4 weeks after cell injections, inflated with PBS, and frozen in Optimal Cutting Temperature compound for analysis by SCOM.

Immunofluorescence staining

Cells were cultured in eight-well chamber glass slides fixed and blocked as previously described (20). The primary antibodies used were as follows: Armenian hamster monoclonal antibody to Intβ1-(FITC) (Abcam), Rabbit polyclonal to FAK ^{Y397} (Abcam), antibody against diphosphorylated MLC (kindly provided by Dr. Sabina Jankowska, Eisai London Research Laboratories, London, United Kingdom; ref. 25), phospho-ERK1/ERK2 (Cell Signaling Technology), and Alexa-Fluor 488 Phalloidin (Molecular Probes). For Src ^{Y416} and FAK^{Y397} costaining, cells were blocked and stained with M.O.M kit FMK-2201 (Vector laboratories, Inc.) and incubated with Src^{Y416} monoclonal antibody (9A6; Assay Designs). For cell viability staining, Calcein AM staining (Trevigen, Inc.) was used according to the manufacturer's protocol. For Col-I staining, frozen lung sections were prepared as previously described (20) and incubated with goat anti–Col-I (1:100; SouthernBiothec).

Statistical analyses

Student's *t* test was used for proliferation assays. For the statistical analyses of metastatic lesion measurements by SCOM, the pixel counts of GFP-positive metastatic lung lesions were quantified for the entire surface area of each lung. Lesions with >10 and <1,000 pixels represented individual tumor cells; lesions with >1,000 pixels represented multicellular metastatic lesions. Total tumor burden/lung was represented by the total number of pixels detected on the entire surface of each lung. Average tumor burden/lung was represented as the median size of the metastatic lesions. Single-cell lesions (<1,000 pixels) and multicellular clusters (>1,000 pixels) were quantified, and the distribution of the sizes of metastatic lesions (represented by the number of pixels per lesion) per lung was calculated. Statistical analyses of differences in the distribution of tumor burden and metastatic lesion size between groups used unpaired Student's *t* test for two-group comparisons and one-way ANOVA planned comparisons for multiple groups. The contrast comparisons tested the differences between fibrotic lungs versus normal lungs for each cell line, and between fibrotic lungs in the different cell lines, after subtracting the control baseline value of the normal lungs for each cell line. Both unadjusted and Bonferroni corrected *P* values were determined and considered significant if <0.05.

Results

Fibrosis triggers metastatic outgrowth of dormant D2.0R cells

Mice instilled with Ad-TGFβ1 developed fibrosis by 3 weeks with extensive deposition of matrix including Col-I, whereas mice treated with Ad-empty or left nontreated did not develop fibrosis (Supplementary Figs. S1 and S2A; Fig. 1A). Twenty-one days after viral transduction, after virus clearance and absence of exogenous viral TGFβ1 expression (24, 26), D2.0R-GFP cells were injected through the tail vein into all three mice groups. Lungs were removed 4 weeks later (Supplementary Fig. S1), and tumor cells in the lungs were imaged by SCOM (Fig. 1B–D). Because initial experiments showed that the growth of D2.OR-GFP cells in the Ad-empty–instilled lungs and nontreated lungs was not significantly different (Supplementary Fig. S2B–D), subsequent experiments were conducted using either Ad-empty– or Ad-TGFβ1–treated mice.

Mice with fibrotic lungs (Ad-TGFβ1) exhibited a significant increase in proliferative metastatic lesions with a marked increase in collagen deposition (Fig. 1A) compared with Ad-empty control mice (Fig. 1B–D). Total tumor burden per lung was 18-fold higher in mice with fibrotic lungs (6.3×10^6 pixels) compared with mice that received null vector (3.5×10^5 pixels; $P \leq 0.001$; Fig. 1B). The average size of the metastatic lesions was 18-fold higher in mice with fibrotic lungs (2.3×10^5 pixels) compared with mice receiving Ad-empty (1.3×10^4 pixels; $P \leq 0.01$; Fig. 1C). Multicellular metastatic lesions and individual metastatic cells expressing GFP were quantified on the entire lung surface. Fluorescence density of >1,000 pixels represented multicellular, proliferative metastatic lesions, whereas foci of <1,000 pixels indicated individual, dormant metastatic cells (Fig. 1D, inset). A percentage the foci (79 ± 3.3%) in fibrotic lungs were multicellular lesions, with only 21 ± 3.3% of the foci persisting as single, quiescent cells. In contrast, only 40 ± 10.8% of the lung lesions were multicellular in mice without fibrosis ($P \leq 0.01$), whereas 60 ± 10.8% of the lung lesions persisted as single quiescent cells (Fig. 1D).

Although Ad-TGFβ1 vector no longer produces TGFβ1 at the time of cell injections into mice, we wished to determine whether TGFβ1 might be capable of initiating the dormant-to-proliferative switch. D2.0R cells cultured in three dimension with BME remained quiescent and did not proliferate in response to TGFβ1. Interestingly, TGFβ1 slightly increased the proliferation of D2.0R cells, which were induced to proliferate with Col-I. (Supplementary Fig. S2E and F). These results strongly suggest that TGFβ1 is not an initiating factor to induce the proliferation of dormant D2.0R cells *in vivo* but may augment their proliferative response after induction of the dormant-to-proliferative switch by Col-I.

Col-I triggers the transition from dormancy to proliferation through Intβ1

Given that Col-I is enriched in the fibrotic environment, we explored whether this ECM protein might play a direct role in the dormant-to-proliferative switch. D2.0R and D2A1 cells were either cultured on BME or on BME+Col-I. Although D2.0R and D2A1 cells cultured in BME alone displayed a rounded morphology at 24 hours, both cell lines cultured in BME+Col-I acquired a flattened, spindle morphology within 24 hours (Supplementary Fig. S4A). D2.0R cells in BME remained quiescent during the 9-day assay period, whereas D2.0R cells cultured in BME + Col-I proliferated within 24 hours ($P \leq 0.0001$; Fig. 2A). Similarly, supplementation of BME with Col-I accelerated the transition from quiescence to proliferation of D2A1 cells ($P \leq 0.0001$; Fig. 2A).

Because Intβ1 serves as a receptor for Col-I, we examined whether the Col-I–induced dormant-to proliferative

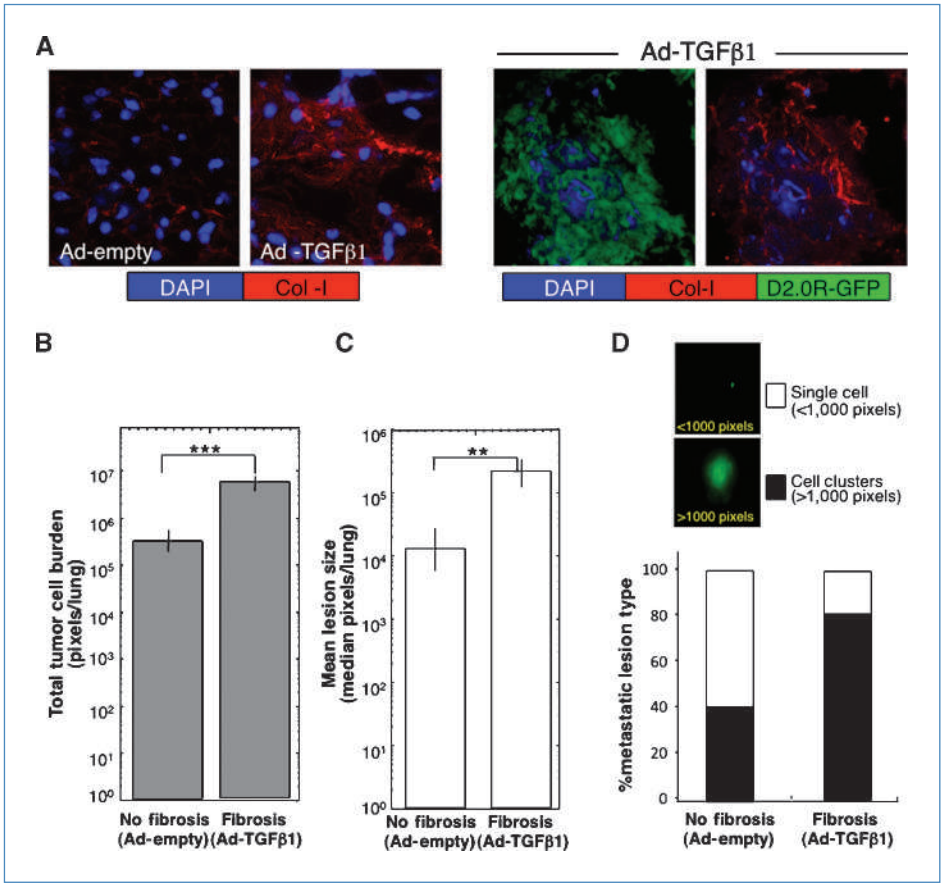

Figure 1. Fibrosis induces the dormant-to-proliferative switch of D2.0R cells in the lung. A, left, lung sections of Ad-empty–treated (no fibrosis) and Ad-TGFβ1–treated (fibrosis) mice stained for Col-I (red). Right, metastatic outgrowth of D2.0R-GFP cells (green) in fibrotic lungs stained for Col-I (red; immunofluorescence, confocal microscopy, X63). B, total D2.0R-GFP tumor cell burden/lung in fibrotic lungs (n = 5) compared with nonfibrotic lungs (n = 5; ***, $P \leq 0.001$). C, average size of metastatic lesions/lung in fibrotic lungs (n = 5) compared with nonfibrotic lungs (n = 5; **, $P \leq 0.01$). D, percentage of single cells versus multicellular proliferative metastatic lesions in nonfibrotic (n = 5) and fibrotic lungs (n = 5). Insert, SCOM images of D2.0R-GFP lung lesions in mice, ×100.

switch was dependent on Intβ1 expression. sh-Intβ1 or sh-NT control was stably expressed in pooled and selected clones of D2.0R cells (dormant phenotype) and D2A1 (metastatic) cells (Fig. 2B). Both D2.0R and D2A1 cells with reduced Intβ1 expression were significantly less responsive to Col-I–induced proliferation ($P \leq 0.0001$; Fig. 2C and D) than parental cells or cells with the nontarget shRNA vector. As shown for quiescent D2.0R cells cultured on BME, quiescent D2.0R and D2A1 cells with reduced Intβ1 expression remained viable as shown by calcein AM staining while maintaining a rounded morphology when cultured on BME+Col-I (Supplementary Fig. S4B).

Intβ1 mediates the switch of solitary dormant D2.0R tumor cells to metastatic growth *in vivo*

Mice were tail vein injected with D2.0R-GFP cells expressing shRNA for Intβ1 (clone #47-6,D2.0R-sh-Intβ1), or D2.0R-GFP expressing nontarget shRNA (D2.0R- sh-NT). Lungs were removed 4 weeks postinjection and analyzed by SCOM (Fig. 3A–C). Metastatic burden in the lungs was analyzed by ANOVA in relation to both presence or absence of fibrosis and the Intβ1 expression (Fig. 3A). A significant 5-fold difference in the total tumor burden/lung in mice with fibrotic lungs receiving D2.0R sh-nontarget cells (sh-NT) compared with mice with nonfibrotic lungs was observed [n = 8; P = 0.018 unadjusted, P = 0.05 with Bonferroni correction (BFC)]. Importantly, no difference was observed in total burden between normal and fibrotic lungs receiving D2.0R-sh-Intβ1 cells (sh-Intβ1; n = 10; P = 0.89 unadjusted, P = 1 with BFC), indicating that fibrosis is associated with significant induction of metastatic lesions that could be prevented by the loss of Intβ1 expression in D2.0R cells. Viable single dormant cells were observed in these lungs, suggesting that the reduction in metastatic burden was not due to the lack of cell viability as a result of the reduction in Intβ1 expression, in keeping with the *in vitro* results above (Supplementary Fig. S4B). Comparing the fibrosis effect only revealed that in fibrotic lungs, the total tumor burden per lung of D2.0R-sh-NT cells was 5-fold higher then the total tumor burden/lung of D2.0R cells with low expression of Intβ1 (sh-Intβ1; Fig. 3A). However, this did not reach statistical significance (P = 0.086 unadjusted, P = 0.26 with BFC) due to the higher error variance when the previous two class comparisons were directly compared.

The average size of metastatic lesions in the fibrotic lungs was significantly higher for D2.0R-sh-NT lesions (3.1×10^5 pixels) compared with D2.0R-sh-Intβ1 lesions (812 pixels; $P \leq 0.05$; Fig. 3B). Similarly, the average size of the metastatic lesions of D2.0R-sh-NT cells in the fibrotic lungs was significantly higher compared with D2.0R-sh-NT

cell lesions in nonfibrotic lungs ($P \leq 0.001$; Fig. 3B). Importantly, as shown in Fig. 3C, the majority of D2.0R-sh-Intβ1 cells persisted as single cells in lungs with or without induced fibrosis (82% ± 12.5% and 97% ± 3.3%, respectively, P = not significant). In contrast, mice with preexisting lung fibrosis and D2.0R-sh-nontarget cells had only 7 ± 4.2% single-cell foci and 93 ± 4.2% proliferative, multicellular foci compared with mice with fibrotic lungs injected with D2.0R-sh-Intβ1 cells exhibiting only 18% ± 12.5% proliferative foci ($P \leq 0.01$; Fig. 3C).

Similar results were obtained using metastatic D2A1 cells with reduced Intβ1 expression (Supplementary Fig. S5A–C). Furthermore, the metastatic lesions that developed from D2A1 sh-nontarget-GFP cells in normal lungs exhibited significant expression of Col-I, whereas regions in the same lungs without D2A1 metastatic lesions did not exhibit significant Col-I expression (Supplementary Fig. S5D), further highlighting the association between proliferative growth and Col-I expression for D2A1 cells.

Intβ1 activation by Col-I induces the phosphorylation of Src and FAK

Interactions between FAK and Src are known to mediate integrin signaling (27). Within 24 hours, D2.0R cells on BME+Col-I proliferated with an associated increase in FAK^{Y397} phosphorylation, which colocalized with Intβ1. These changes were absent in cells cultured only on BME (Supplementary Figs. S6A and S7A). Inhibition of Intβ1 in D2.0R cells cultured on BME+Col-I with either αIntβ1 antibody (αIntβ1Ab) or shRNA led to a marked reduction in both in $pFAK^{Y397}$ and colocalization with Intβ1 compared with controls (Supplementary Figs. S6B and C and S7A and B). BME+Col-I significantly enhanced the phosphorylation and colocalization of $pSrc^{Y416}$ and $pFAK^{Y397}$ in D2.0R cells (Fig. 4A).

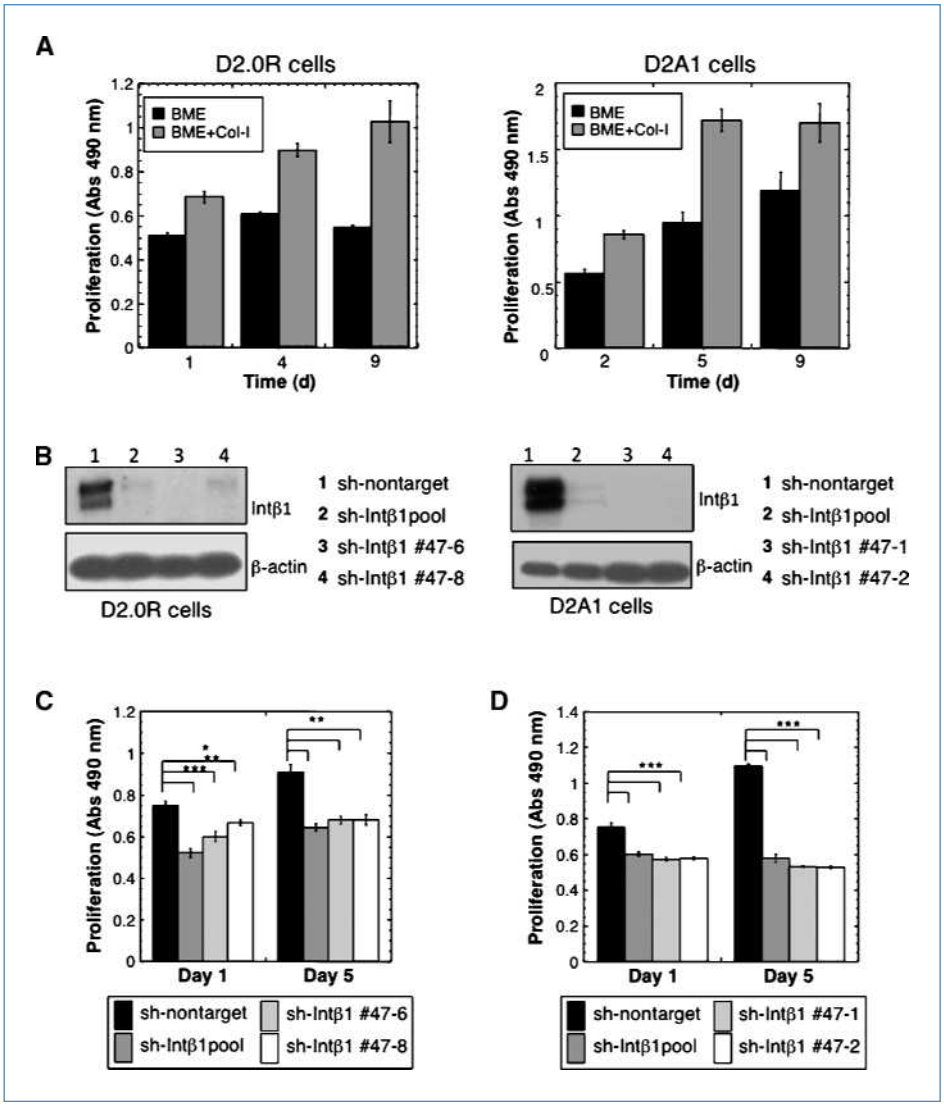

Figure 2. Col-I induces the transition from quiescence to proliferation of D2.0R and D2A1 cells through Intβ1. A, proliferation of D2.0R and D2A1 cells in BME+Col-I, compared with cells grown in BME (columns, mean; bars, SEM; $n = 8$; $P \leq 0.0001$). B, Western blot for Intβ1 expression. Left, D2.0R cell lines. Right, D2A1 cell lines. C and D, proliferation of D2.0R (C) and D2A1 cells (D) in BME+ Col-I (columns, mean; bars, SEM; $n = 8$; *, $P \leq 0.05$; **, $P \leq 0.01$; ***, $P \leq 0.0001$). Representative results of three independent experiments for all data shown.

Inhibition of Src activity in D2.0R cells cultured on BME+Col-I using the inhibitor PP1 or Src shRNA (Supplementary Fig. S8) prevented the phosphorylation of FAK^{Y397}, colocalization with Intβ1 (Fig. 4B), and proliferation ($P \leq 0.0001$; Fig. 4D). Inhibition of Intβ1 with αInt β1AB or shRNA significantly reduced p FAK^{Y397} and p Src^{Y416} and their colocalization compared with controls (Supplementary Fig. S7A and B; Fig. 4C).

FAK and Src activate ERK leading to proliferation (28). Quiescent D2.0R cells cultured on BME had minimal activated ERK (pERK; Supplementary Fig. S7A; Fig. 5A). The increased pERK, actin stress fiber formation, and proliferation in D2.0R cells cultured on BME+Col-I (Fig. 5A) were inhibited with αIntβ1AB (Fig. 5B), Intβ1 shRNA (Supplementary Fig. S7A and B; Fig. 5C), or through inhibition of Src activity with PP1 or Src shRNA (Fig. 5D). Scrambled shRNA had no effect (data not shown).

Col-I–induced Intβ1 signaling activates ERK, leading to pMLC by MLCK and actin stress fiber formation

The dormant-to-proliferative switch of D2.0R cells requires actin stress fiber formation through the pMLC by MLCK (20), which can be regulated by ERK (29). D2.0R cells in BME+Col-I showed a marked increase in pMLC and actin stress fibers (Supplementary Fig. S7A; Fig. 6A) compared with BME alone. Inhibition of MLCK directly by ML-7 (30) or through inhibition of upstream signaling molecules that regulate MLCK activity (ERK using U-0126 or Ca2+ calmodulin using W13) reduced pMLC, inhibited actin stress fiber formation, and inhibited proliferation ($P \leq 0.0001$; Fig. 6A and B). Inhibiting Intβ1 function also reduced pMLC and actin stress fiber formation compared with controls (Supplementary Fig. S7A; Fig. 6C). Inhibiting Src activity with PP1 or shRNA also reduced pMLC, actin stress fiber formation (Fig. 6D), and proliferation.

Discussion

Our results indicate that tumor cells already carrying critical genetic alterations can remain dormant or can be triggered to proliferate by changes occurring in their microenvironment. Thus, tumor dormancy may be maintained in an initially nonpermissive microenvironment, but transition to a proliferative state may result from extrinsic changes within the microenvironment. This study shows *in vivo* for the first time how changes in the ECM composition produced by stromal cells can initiate the transition of solitary dormant cells to metastatic proliferation. Several gene expression studies have identified ECM-related genes (including Col-I) in prognostic signatures for poor outcome, metastases, and tumor recurrence (13, 15). In this study, we show that an *in vivo* fibrotic environment that contains high amounts of Col-I, as well as other ECM proteins, may induce the transition from a dormant-to-proliferative state through Intβ1. Mice with fibrotic lungs displayed greatly increased numbers and sizes of proliferative, metastatic lesions compared with mice without fibrosis.

Intβ1 is the primary receptor that interacts with Col-I. Previous studies have reported the important role of Intβ1 in

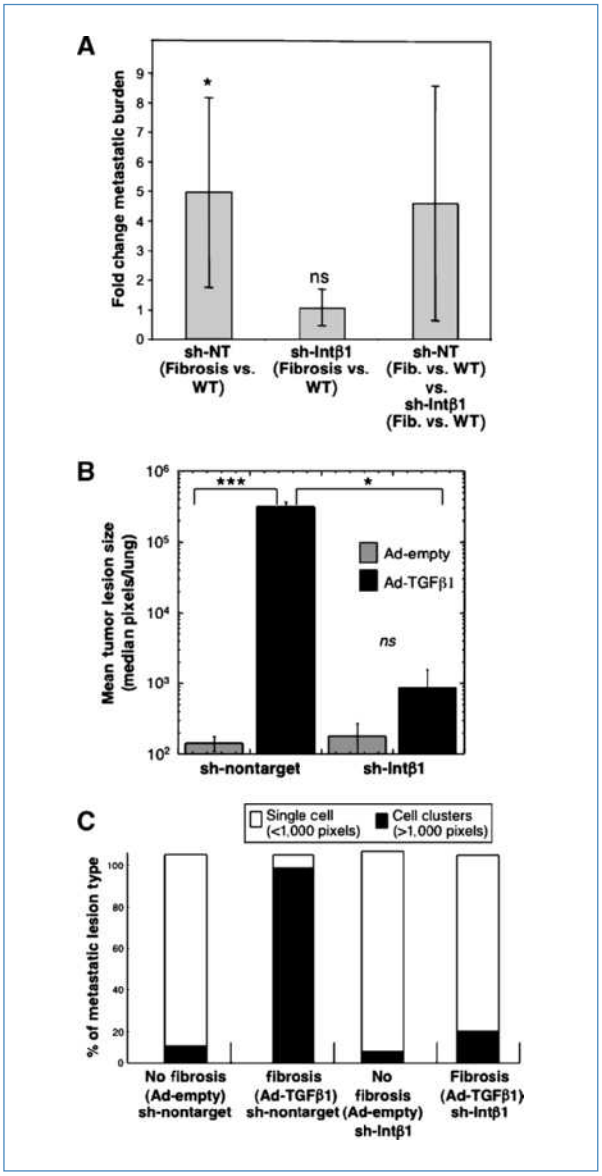

Figure 3. Loss of Intβ1 expression inhibits the fibrosis-induced transition from dormancy to metastatic outgrowth in mice. A, fold difference in total tumor burden per lung for each cell line in response to fibrosis (total pixels in fibrotic lungs/total pixels in nonfibrotic lungs). Fibrosis significantly increases total tumor burden/lung of D2.0R-sh-NT cells compared with nonfibrotic lungs (*, $P = 0.018$ unadjusted, $P = 0.05$ with BFC), whereas inhibition of Intβ1(sh-Intβ1) abolishes the response to fibrosis (no significant difference, $P = 0.89$ unadjusted, $P = 1$ with BFC). [sh-NT - sh-Intβ1], the comparison between the sh-NT class analysis versus sh-Intβ1 analysis (ns, not significant). B, average size of the metastatic lesions in fibrotic lungs (Ad-TGFβ) from D2.0R-GFP- sh-NT cells and D2.0R-GFP-sh-Intβ1 cells (*, $P = 0.00014$ uncorrected; $P = 0.00042641$ with BFC) as well as for D2.0R-GFP-sh-nontarget (sh-NT) cells in nonfibrotic lungs (Ad-empty; $P = 0.013$ unadjusted; $P = 0.039$ with BFC). C, percentage of single cells versus proliferative metastatic lesions in nonfibrotic versus fibrotic lungs of D2.0R-GFP-sh-NT or D2.0R-GFP sh-Intβ1 cells. D2.0R-GFP- sh-NT cells had a significantly higher percentage of multicellular, proliferative lesions in fibrotic lungs compared with D2.0R-GFP-sh-Intβ1 cells ($P = 0.001$ uncorrected; $P = 0.003$ with BFC) as well as for D2.0R-GFP- sh-NT cells in nonfibrotic lungs ($P = 1.75E-05$ uncorrected; $P = 5.25E-05$ with BFC).

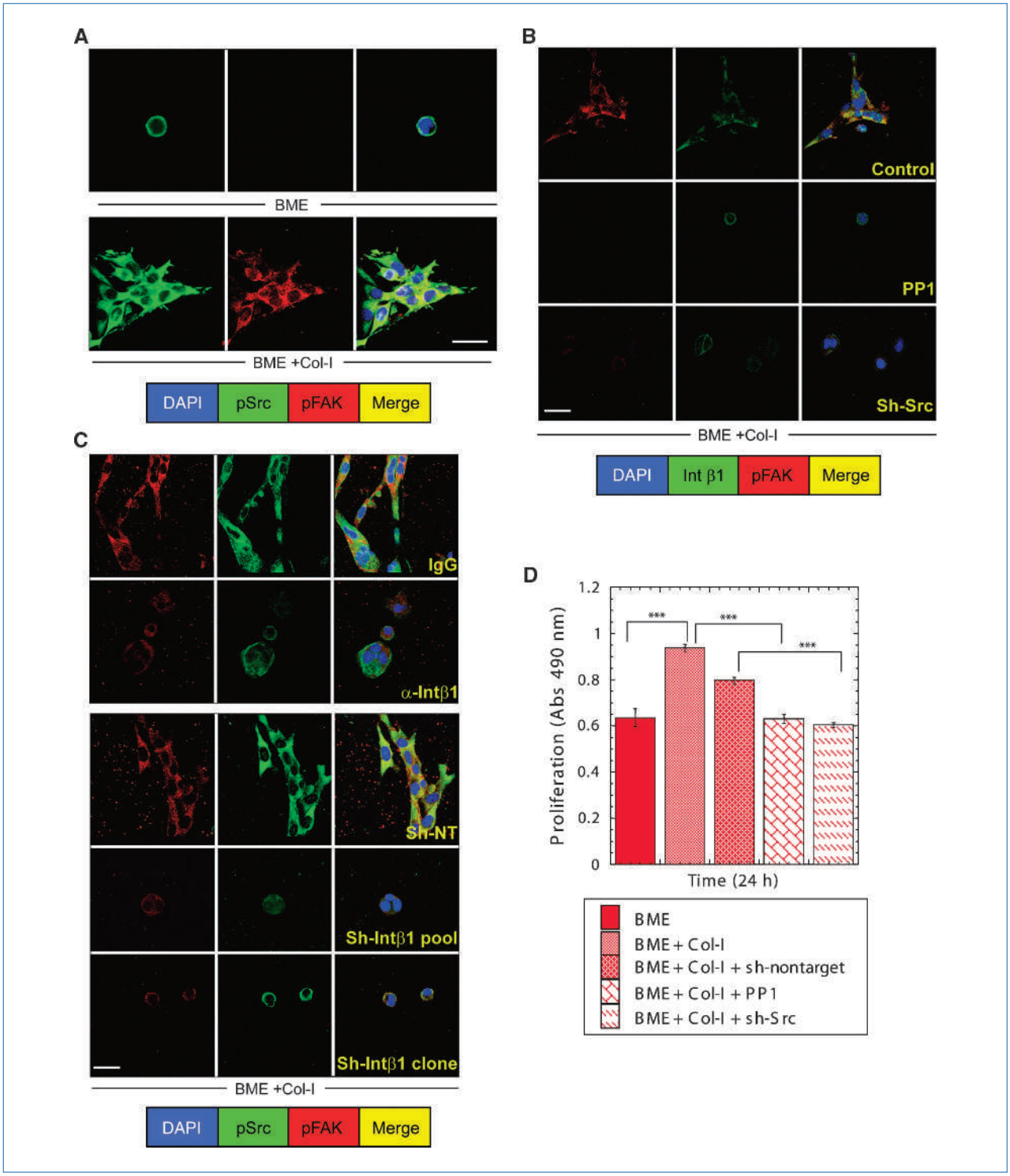

Figure 4. Src activation is required for Col-I-induced FAK^{Y397} phosphorylation and the transition from quiescence to proliferation of D2.0R cells. A and C, coimmunofluorescence staining for Src^{Y416}, FAK^{Y397}, and nuclear staining with 4′,6-diamidino-2-phenylindole (DAPI). A, cells cultured on BME and BME+Col-I for 24 h. B, coimmunofluorescence staining for Intβ1, FAK^{Y397}, and nuclear staining with DAPI of D2.0R cells cultured on BME+Col-I for 24 h treated either with PP1 (10 μmol/L) or sh-Src. C, D2.0R cells cultured on BME+Col-I for 24 h with nonspecific IgG (100 μg/mL) or D2.0R nontarget shRNA cells or D2.0R cells treated with anti-Intβ1 antibody (100 μg/mL) or pooled D2.0R cells and D2.0R-sh-Intβ1 cells. D, proliferation of D2.0R cells in BME or BME+Col-I with or without 10 μmol/L PP1, nontarget shRNA, or sh-Src (n = 8; columns, mean; bars, SEM; $P \leq 0.0001$). Confocal microscopy, ×63; Scale bars, 20 μm. Representative of three independent experiments.

different stages of tumor progression (31–35). We showed that Intβ1 is a key regulator in the switch from dormancy to metastatic growth. Reduced expression of Intβ1 in D2.0R cells disseminated to preexisting fibrotic lungs resulted in a 5-fold reduction in proliferative metastatic lesions compared with control cells. Similarly, in the context of a normal lung environment, loss of Intβ1 expression in metastatic D2A1 cells resulted in a 9-fold reduction of metastatic lesions and lower tumor burden compared with D2A1-sh-NT cells. Metastatic lesions arising from D2A1 cells in nonfibrotic lungs were associated with significant deposition of Col-I, suggesting that the metastatic D2A1 cells are able to induce a Col-I stromal response to stimulate their growth, whereas D2.0R cells require an exogenous fibrotic stimulus to initiate their proliferative response. Previous studies in head and neck carcinoma have shown critical cross-talk between urokinase receptor and Intβ1 in tumor dormancy (36, 37). We have determined that Col-I increases Intα1 mRNA, but not α2 or α7 integrin in D2.0R cells *in vitro*, suggesting that α1β1 is the most likely candidate Col-I receptor on D2.0R cells (data no shown).

Based on our previous study, fibronectin may also contribute to the dormant-to-proliferative switch in this *in vivo* fibrosis model system because fibronectin also activates Intβ1 in D2.0R and D2A1 cells (20). Although we do not exclude the influences of other factors in the microenvironment of the fibrotic lungs, such as a possible role of

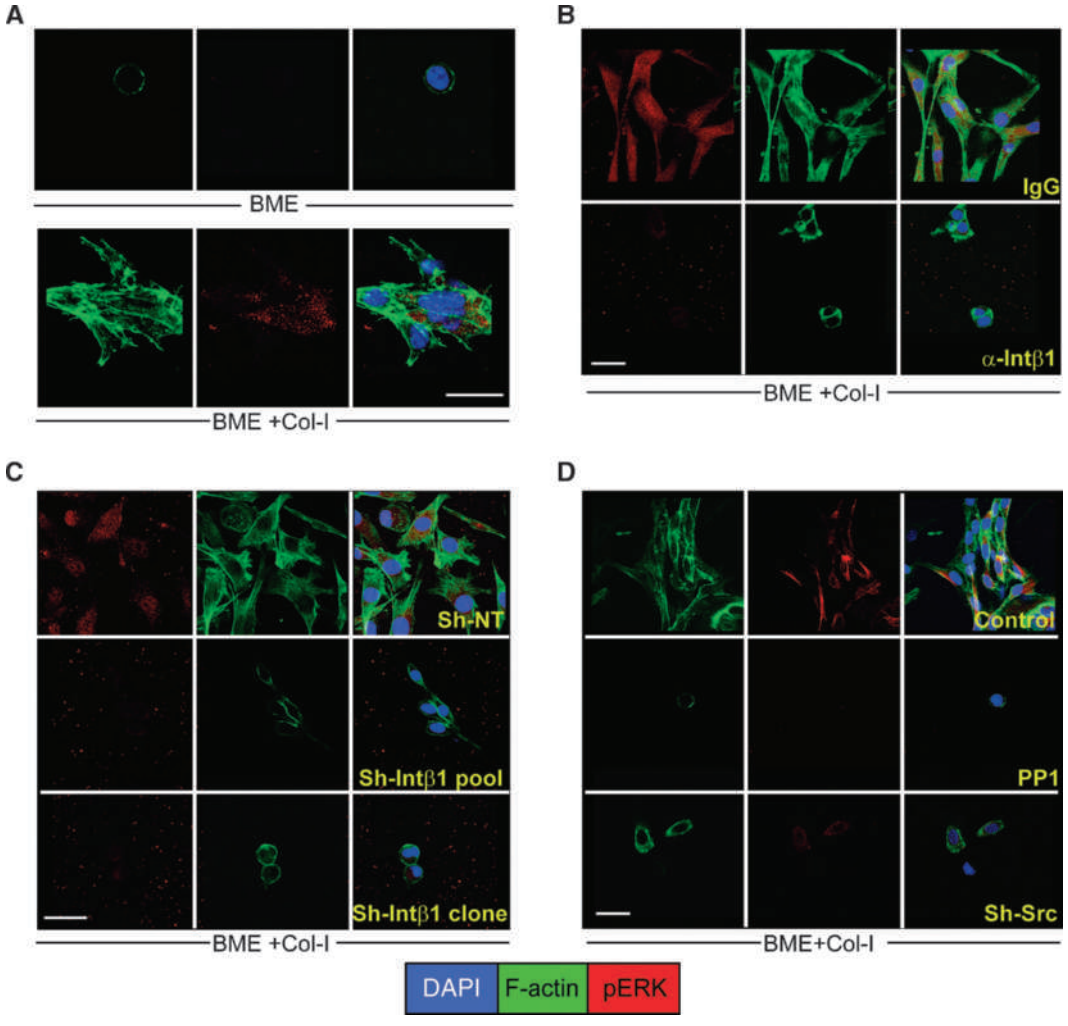

Figure 5. Col-I induces actin stress fiber formation and activation of ERK through Intβ1 and Src. A to D, coimmunofluorescence staining of D2.0R cells for pERK, filamentous actin (F-actin) with phalloidin, and nuclear staining with DAPI after (A) 24 h culture on BME or BME +Col-I, (B) D2.0R cells on BME+Col-I treated with nonspecific IgG (100 μg/mL) or anti-Intβ1 antibody (100 μg/mL), (C) sh-nontarget and sh-Intβ1, or (D) 10 μmol/L PP1 or sh-Src. Confocal microscopy ×63; scale bars, 20 μm. Representative of three independent experiments.

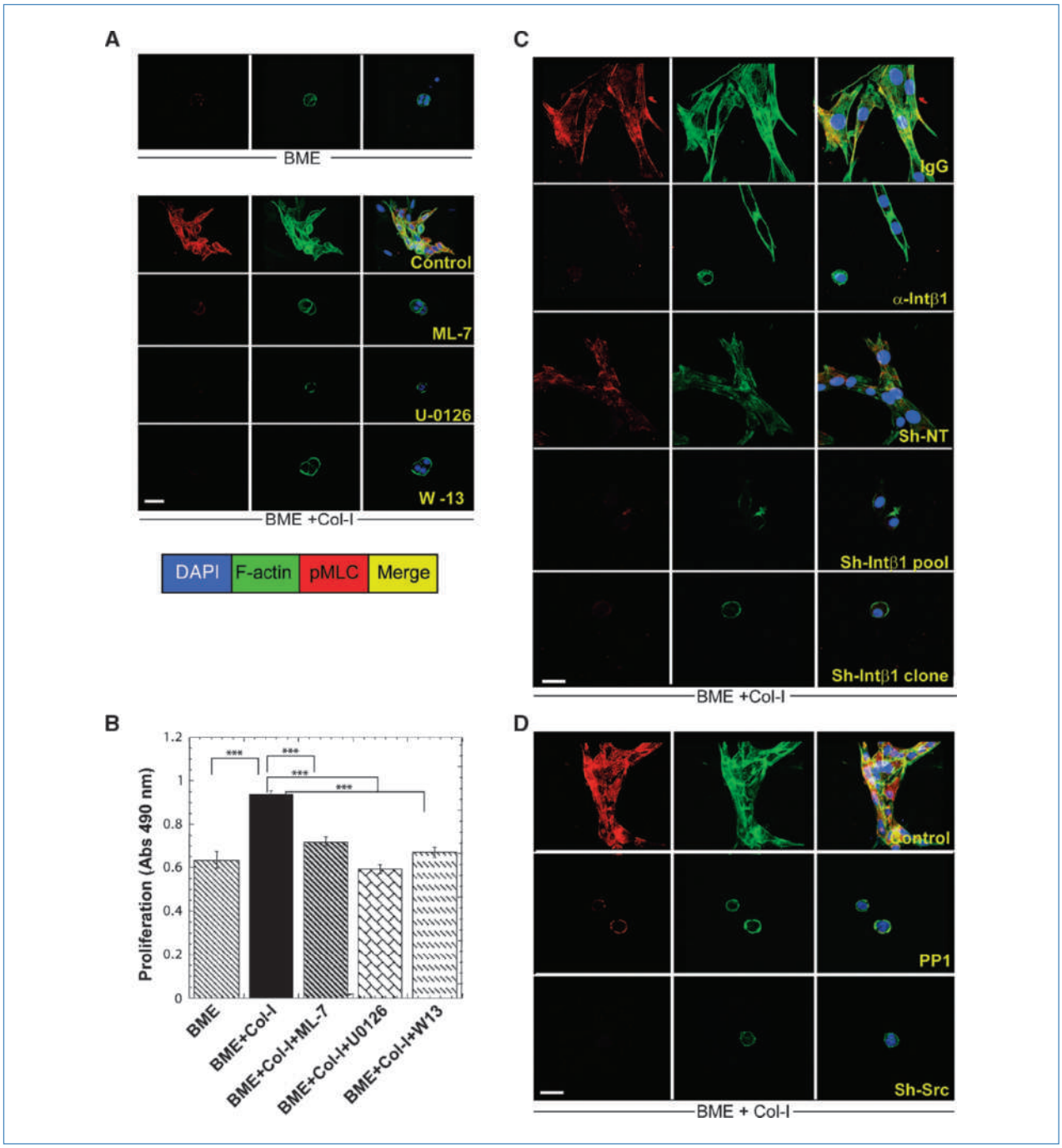

Figure 6. Col-I–mediated signaling through Intβ1 induces pMLC by MLCK leading to proliferation of quiescent cells. A, coimmunofluorescence staining for phospho-MLC, F-actin, and nuclear localization with DAPI of D2.0R cells cultured for 24 h on BME or BME+Col-I either nontreated or treated with ML-7 (5 μmol/L), U-0126 (10 μmol/L), or W-13 (10 μmol/L). B, proliferative response to Col-I with or without inhibitors (n = 8; columns, mean; bars, SEM; $P \leq 0.0001$). C, D2.0R cells on BME+Col-I with nonspecific IgG (100 μg/mL), anti-Intβ1 antibody (100 μg/mL), and D2.0R cells stably expressing nontarget-shRNA and D2.0R sh-Intβ1cells (pooled or clone #47-6). D, D2.0R cells cultured on BME+Col-I (control) or treated with 10 μmol/L PP1, or sh-Src. Confocal microscopy ×63; scale bars, 20 μm. Representative results of three independent experiments.

TGFβ in sustaining/enhancing the proliferation of the emerging micrometastasis, our results using the three-dimensional *in vitro* model system for dormancy (20) showed that a signaling cascade induced by Col-I is sufficient to trigger the dormant-to-proliferative switch of D2.0R cells through activation of Intβ1, Src, FAK, and ERK leading to pMLC by MLCK, and actin stress fiber formation—all critical for the proliferative response.

Our previous study showed the critical role of actin stress fiber formation in the transition from dormancy to proliferative growth. In this study, we have further shown that actin stress fiber formation is regulated through Col-I activation and is dependent on Intβ1, FAK, Src, and ERK, a key regulator of the cell cycle and MLCK (29), which phosphorylates MLC leading to actin stress fiber formation. Furthermore, we showed that activated ERK is critical for actin stress fiber formation through pMLC by MLCK, required for the transition from quiescence to proliferation.

Our results are consistent with several clinical correlations between enriched stromal Col- I and cancer recurrence and reduced survival. Women with high breast density, associated with enriched stromal Col-I, have an increased risk for local recurrence after mastectomy or radiotherapy (38). Fibrotic foci are found around some invasive ductal carcinomas and their recurring lesions residing at lymph nodes and bones. Notably, patients with fibrotic foci are at higher risk of developing bone and lymph node metastasis, and disease recurrence (17, 39). Osteosclerotic breast cancer bone metastases exhibit marrow fibrosis and new bone formation (40). Therefore, enriched stromal Col-I in a more fibrotic microenvironment or induced by the residing tumor cells may provide a fertile "soil" for the transition from dormancy to metastatic growth.

In summary, we have shown for the first time, to our knowledge, how fibrosis with Col-I enrichment may serve as a critical element in modifying the soil of metastatic sites and activating dormant tumor cells to proliferate. These results suggest that inhibiting the interaction between dormant tumor cells and growth-promoting changes in the ECM that signal through Intβ1 may be an important new avenue to prevent disease recurrence.

Disclosure of Potential Conflicts of Interest

No potential conflicts of interest were disclosed.

Acknowledgments

We thank Drs. Marry Ann Step, Glenn Merlino, and Peter Blumberg for valuable discussions; Dr. Chand Khanna for the use of SCOM equipment; the LRBGE Fluorescence Imaging Core; and Anthony Vieira and Dr. Zi-Yao Liu for the technical assistance.

Grant Support

This research was supported by the Intramural Program of NIH, Center for Cancer Research, National Cancer Institute, and the Canadian Institutes of Health Research.

The costs of publication of this article were defrayed in part by the payment of page charges. This article must therefore be hereby marked *advertisement* in accordance with 18 U.S.C. Section 1734 solely to indicate this fact.

Received 06/25/2009; revised 04/17/2010; accepted 05/11/2010; published OnlineFirst 06/22/2010.

References

1. Pantel K, Schlimok G, Braun S, et al. Differential expression of proliferation-associated molecules in individual micrometastatic carcinoma cells. J Natl Cancer Inst 1993;85:1419–24.
2. Braun S, Vogl FD, Naume B, et al. A pooled analysis of bone marrow micrometastasis in breast cancer. N Engl J Med 2005;353:793–802.
3. Townson JL, Chambers AF. Dormancy of solitary metastatic cells. Cell Cycle 2006;5:1744–50.
4. Wikman H, Vessella R, Pantel K. Cancer micrometastasis and tumour dormancy. APMIS 2008;116:754–70.
5. Aguirre-Ghiso JA. Models, mechanisms and clinical evidence for cancer dormancy. Nat Rev Cancer 2007;7:834–46.
6. Holmgren L, O'Reilly MS, Folkman J. Dormancy of micrometastases: balanced proliferation and apoptosis in the presence of angiogenesis suppression. Nat Med 1995;1:149–53.
7. Naumov GN, Bender E, Zurakowski D, et al. A model of human tumor dormancy: an angiogenic switch from the nonangiogenic phenotype. J Natl Cancer Inst 2006;98:316–25.
8. Fidler IJ. The organ microenvironment and cancer metastasis. Differentiation 2002;70:498–505.
9. Bissell MJ, Radisky DC, Rizki A, Weaver VM, Petersen OW. The organizing principle: microenvironmental influences in the normal and malignant breast. Differentiation 2002;70:537–46.
10. Hu M, Polyak K. Microenvironmental regulation of cancer development. Curr Opin Genet Dev 2008;18:27–34.
11. Schedin P, Elias A. Multistep tumorigenesis and the microenvironment. Breast Cancer Res 2004;6:93–101.
12. Massague J. New concepts in tissue-specific metastases. Clin Adv Hematol Oncol 2003;1:576–7.
13. Ramaswamy S, Ross KN, Lander ES, Golub TR. A molecular signature of metastasis in primary solid tumors. Nat Genet 2003;33:49–54.
14. Qiu TH, Chandramouli GV, Hunter KW, Alkharouf NW, Green JE, Liu ET. Global expression profiling identifies signatures of tumor virulence in MMTV-PyMT-transgenic mice: correlation to human disease. Cancer Res 2004;64:5973–81.
15. Calvo A, Catena R, Noble MS, et al. Identification of VEGF-regulated genes associated with increased lung metastatic potential: functional involvement of tenascin-C in tumor growth and lung metastasis. Oncogene 2008;27:5373–84.
16. Ma XJ, Dahiya S, Richardson E, Erlander M, Sgroi DC. Gene expression profiling of the tumor microenvironment during breast cancer progression. Breast Cancer Res 2009;11:R7.
17. Hasebe T, Sasaki S, Imoto S, Mukai K, Yokose T, Ochiai A. Prognostic significance of fibrotic focus in invasive ductal carcinoma of the breast: a prospective observational study. Mod Pathol 2002;15:502–16.
18. Van den Eynden GG, Smid M, Van Laere SJ, et al. Gene expression profiles associated with the presence of a fibrotic focus and the growth pattern in lymph node-negative breast cancer. Clin Cancer Res 2008;14:2944–52.
19. Jensen BV, Johansen JS, Skovsgaard T, Brandt J, Teisner B. Extracellular matrix building marked by the N-terminal propeptide of procollagen type I reflect aggressiveness of recurrent breast cancer. Int J Cancer 2002;98:582–9.
20. Barkan D, Kleinman H, Simmons JL, et al. Inhibition of metastatic outgrowth from single dormant tumor cells by targeting the cytoskeleton. Cancer Res 2008;68:6241–50.
21. Morris VL, Koop S, MacDonald IC, et al. Mammary carcinoma cell lines of high and low metastatic potential differ not in extravasation but in subsequent migration and growth. Clin Exp Metastasis 1994;12:357–67.
22. Naumov GN, MacDonald IC, Weinmeister PM, et al. Persistence of solitary mammary carcinoma cells in a secondary site: a possible contributor to dormancy. Cancer Res 2002;62:2162–8.
23. Khanna C, Wan X, Bose S, et al. The membrane-cytoskeleton linker

ezrin is necessary for osteosarcoma metastasis. Nat Med 2004;10:182–6.
24. Bonniaud P, Kolb M, Galt T, et al. Smad3 null mice develop airspace enlargement and are resistant to TGF-β-mediated pulmonary fibrosis. J Immunol 2004;173:2099–108.
25. Ratcliffe MJ, Smales C, Staddon JM. Dephosphorylation of the catenins p120 and p100 in endothelial cells in response to inflammatory stimuli. Biochem J 1999;338:471–8.
26. Sime PJ, Xing Z, Graham FL, Csaky KG, Gauldie J. Adenovector-mediated gene transfer of active transforming growth factor-β1 induces prolonged severe fibrosis in rat lung. J Clin Invest 1997;100:768–76.
27. Gabarra-Niecko V, Schaller MD, Dunty JM. FAK regulates biological processes important for the pathogenesis of cancer. Cancer Metastasis Rev 2003;22:359–74.
28. Yee KL, Weaver VM, Hammer DA. Integrin-mediated signalling through the MAP-kinase pathway. IET Syst Biol 2008;2:8–15.
29. Klemke RL, Cai S, Giannini AL, Gallagher PJ, de Lanerolle P, Cheresh DA. Regulation of cell motility by mitogen-activated protein kinase. J Cell Biol 1997;137:481–92.
30. Saitoh M, Ishikawa T, Matsushima S, Naka M, Hidaka H. Selective inhibition of catalytic activity of smooth muscle myosin light chain kinase. J Biol Chem 1987;262:7796–801.
31. White DE, Kurpios NA, Zuo D, et al. Targeted disruption of β1-integrin in a transgenic mouse model of human breast cancer reveals an essential role in mammary tumor induction. Cancer Cell 2004;6:159–70.
32. Paszek MJ, Zahir N, Johnson KR, et al. Tensional homeostasis and the malignant phenotype. Cancer Cell 2005;8:241–54.
33. Park CC, Zhang H, Pallavicini M, et al. β1 integrin inhibitory antibody induces apoptosis of breast cancer cells, inhibits growth, and distinguishes malignant from normal phenotype in three dimensional cultures and *in vivo*. Cancer Res 2006;66:1526–35.
34. Kren A, Baeriswyl V, Lehembre F, et al. Increased tumor cell dissemination and cellular senescence in the absence of β1-integrin function. EMBO J 2007;26:2832–42.
35. Imanishi Y, Hu B, Jarzynka MJ, et al. Angiopoietin-2 stimulates breast cancer metastasis through the α(5)β(1) integrin-mediated pathway. Cancer Res 2007;67:4254–63.
36. Aguirre Ghiso JA, Kovalski K, Ossowski L. Tumor dormancy induced by downregulation of urokinase receptor in human carcinoma involves integrin and MAPK signaling. J Cell Biol 1999;147:89–104.
37. Aguirre-Ghiso JA, Liu D, Mignatti A, Kovalski K, Ossowski L. Urokinase receptor and fibronectin regulate the ERK(MAPK) to p38(MAPK) activity ratios that determine carcinoma cell proliferation or dormancy *in vivo*. Mol Biol Cell 2001;12:863–79.
38. Park CC, Rembert J, Chew K, Moore D, Kerlikowske K. High mammographic breast density is independent predictor of local but not distant recurrence after lumpectomy and radiotherapy for invasive breast cancer. Int J Radiat Oncol Biol Phys 2009;73:75–9.
39. Koyama T, Hasebe T, Tsuda H, et al. Histological factors associated with initial bone metastasis of invasive ductal carcinoma of the breast. Jpn J Cancer Res 1999;90:294–300.
40. Kamby C, Guldhammer B, Vejborg I, et al. The presence of tumor cells in bone marrow at the time of first recurrence of breast cancer. Cancer 1987;60:1306–12.